치의과학박사 학위논문

Effects of Thermocycling treatment on the Mechanical and Chemical Changes of Resin-based Composites in Acidic Environment

열순환 처리가 산성 환경에서의 복합레진의 기계적, 화학적 변화에 미치는 영향

2023년 2월

서울대학교 대학원

치의학과학과 치과보존학 전공

강 승 호

Effects of Thermocycling treatment on the Mechanical and Chemical Changes of Resin-based Composites in Acidic Environment

지도교수 조병훈

이 논문을 치의과학박사 학위논문으로 제출함
2022년 12월

서울대학교 대학원
치의과학과 치과보존학 전공
강 승 호

강승호의 치의과학박사 학위논문을 인준함
2023년 1월

위 원 장 ______________________ (인)

부위원장 ______________________ (인)

위 원 ______________________ (인)

위 원 ______________________ (인)

위 원 ______________________ (인)

The manuscript will be published in the journal

Operative Dentistry 2023.

Abstract

Effects of Thermocycling treatment on the Mechanical and Chemical Changes of Resin-based Composites in Acidic Environment

Seungho Kang, D.D.S, M.S.D
Program in Conservative Dentistry
Department of Dental Science
Graduate School, Seoul National University
(Directed by Prof. Byeong-Hoon Cho, D.D.S., M.S.D., Ph.D.)

Objectives. This study investigated the aging effects of long-term exposure to acidic beverages on the flexural strength (FS) and chemical reactions of two resin-based composites (RBCs, Tetric N-Ceram bulkfil and Z250) and one giomer (Beautifil II).

Materials and Methods. The specimen bars (2 mm × 2 mm × 25 mm) were aged at various levels of thermocycling (TC, 0, 10,000, 50,000, and 100,000 cycles) in two beverages with different pH values (distilled water [DW], pH 7.0; Coca-Cola, pH 2.4-2.8). The aged specimens were subjected to a 4-point bending test. A compressive load was applied using a universal testing machine (LF Plus, Lloyd Instruments, Fareham, UK) at a crosshead speed of 0.5 mm/min. A scanning electron microscopy (SEM, Apreo S, Thermo Fisher Scientific, Waltham, MA, USA) was used to observe the edge adjacent to the fracture margin on the bottom surface under tension and the fractured surface of the specimen bars. Fourier transform infrared spectroscopy in attenuated total reflectance mode (FTIR-ATR) spectra were recorded for Z250 only using an FTIR system (Spectrum 100, PerkinElmer, Waltham, MA, USA). The absorption spectra of each cured specimen were measured four times of TC. X-ray photoelectron spectroscopy (XPS, K-Alpha+, ThermoFisher Scientific, Waltham, MA, USA) analysis was performed to compare changes in the chemical characteristics on the bottom surface of the Z250 specimens under tension between neutral DW and acidic Coca-Cola. The FS data were analyzed using three-way analysis of variance with the *post hoc* Tukey test and t-test at a significance level of α=0.05.

Results. In DW, the FS of an RBC, Tetric N-Ceram Bulk fill, and a giomer, Beautifil II, did not decrease until 10,000 cycles, but significant decreases were observed at 50,000 cycles in both products ($p<0.05$). Although the initial FS of the other RBC, Z250, was higher than those of Tetric N-Ceram Bulk fill and Beautifil II, the FS of Z250 decreased continuously until 50,000 cycles ($p<0.05$), followed by no additional decrease until 100,000 cycles. In Coca-Cola, the FS of all materials decreased more rapidly than in DW from 10,000 cycles (t-test, $p<0.05$). Thereafter, until 100,000 cycles, the FS of Beautifil II and Tetric N-Ceram did not show any statistically significant decrease. However, Z250 showed an increased FS at 100,000 cycles in both aging solutions ($p<0.05$). In the SEM images, as the number of cycles increased, irregularly-shaped larger fillers and more pores were observed on the surfaces of the specimens. For the same number of cycles, more pores were observed in Coca-Cola than in DW. The changes of the hydroxyl group observed at 3340 cm^{-1} and the ester group observed at 1730-1700 cm^{-1} were observed using FTIR-ATR. In DW, no significant change was observed even after TC. In Coca-Cola, the hydroxyl group peak of 3340 cm^{-1} shifted to 3270 cm^{-1} after TC, showing a wider and gentle slope than the before. The easter group observed at 1730-1700 cm^{-1} has a peak shifted to 1733 cm^{-1}, and has changed to a narrower and sharper peak than before. In XPS, a decrease in the C=C peak and an increase in the C-O peak were commonly observed after TC. In DW, the Si-O peak gradually increased compared to the Si-C peak, and in Coke, the Si-O peak increased, but not gradually, and after 100,000 times, it became similar to that of DW.

Conclusion. When TC was performed in DW, unreacted monomers and coupling agent were washed out, which caused porosity and reduced FS. In Coca−Cola, acidic conditions accelerated removal of the matrix through the hydrolytic reaction at the ester groups, resulting in more porosity and a faster decrease in FS than in DW.

Keywords : Aging; Chemical change; Flexural strength;
Resin−based composite; Surface roughness

Student Number : 2019−30042

CONTENTS

Effects of Thermocycling treatment on the Mechanical and Chemical Changes of Resin-based Composites in Acidic Environment

Seungho Kang, D.D.S, M.S.D
Program in Conservative Dentistry
Department of Dental Science
Graduate School, Seoul National University
(Directed by Prof. Byeong-Hoon Cho, D.D.S., M.S.D., Ph.D.)

INTRODUCTION

Resin-based composites (RBCs) have shown continual improvements in their mechanical and esthetic properties. As these materials improve, they are being used to replace amalgams.[1,2] However, RBCs are challenged by various harsh conditions in the oral environment, including chemical, mechanical, and thermal stresses. Although most beverages consist mainly of water, some have adverse chemical and thermal effects on RBCs, depending on the nature of their ingredients, pH, and temperature. Due to the different coefficients of thermal expansion between tooth substrates and restorations, RBCs may also be affected by the ingestion of foods with different temperatures. Repeated exposure to adverse oral environments may cause the matrices of RBCs to dissolve and the fillers to peel off and finally separate at the bonded interface.[3,4]

Most RBCs contain bisphenol A-glycidyl methacrylate (Bis-GMA) and triethylene glycol dimethacrylate (TEGDMA) as matrix monomers, and silane as coupling agent. They have C=C functional groups at their ends and are polymerized by reacting with radicals. The C=C bonds at the end of the ester group can be hydrolyzed under certain conditions. Therefore, RBCs also can be hydrolyzed by continuous exposure to saliva in the oral cavity, and the hydrolysis of dental resin can be accelerated by enzymes and acids. Bonds formed between a coupling agent and an inorganic filler are prone to hydrolysis.[5,6,7] The primary byproduct of the hydrolysis of methacrylates is methacrylic acid (MA). The degradation of Bis-

GMA and TEGDMA results in the formation of bishydroxy-propoxy-phenyl-propane (BisHPPP) and triethylene glycol methacrylate (TEGMA). Further breakdown of TEGMA leads to the creation of triethylene glycol (TEG).[8] Chemical degradation of RBCs results in deterioration of the structure, such as degradation of chemical bonds within matrix and/or between matrix and fillers, and consequently, deterioration of material's mechanical properties.

Giomer and bulk-fill composite resins have different compositions from those of conventional RBCs, including different matrix monomers, fillers, and photoinitiators, which can create varied physical properties and result in different chemical reactions in the oral cavity. Giomers have surface pre-reacted glass-ionomer (S-PRG) fillers that exert antimicrobial activity against *Streptococcus mutans* by releasing multiple ions from the glass-ionomer phase formed in the filler. This material combines the fluoride-releasing abilities of a resin-modified glass ionomer and the improved physical properties of a composite resin.[9,10,11,12] Because S-PRG fillers contain a variety of elements, the properties of giomers may be affected by the bonding between matrices and fillers; therefore, aging may affect the strength of giomers. The mechanical properties of bulk-fill composite resins have been debated. Some authors have reported that the values of their mechanical properties were lower than those of conventional RBCs, while others reported that the values were close to those of conventional RBCs.[13,14]

Among the various beverages that are widely consumed around the world, Coca-Cola is one of the most destructive beverages to the dentition. It has a low pH (2.4~2.8) and it is known to corrode tooth substrates and intraoral restorations because it contains highly acidic carbonic acid.[15,16] Coca-Cola also contains several ingredients that have demonstrated complicated reactions with oral biofilm, tooth substrates, and dental materials. The high level of sugar in Coca-Cola also acts as a nutrient for the growth of oral bacteria. Therefore, it is thought that frequent consumption of Coca-Cola may increase the incidence of dental caries, and many studies have used Coca-Cola as a reference drink that can cause dental caries.[17,18] Several studies have also observed that the mechanical properties of resins decreased when exposed to beverages that contained corrosive chemicals, affecting the durability and longevity of the resins.[19,20,21,22]

Thermocycling (TC) is an experimental method that places materials in alternating hot and cold liquids. As a result, the material repeatedly contracts and expands and undergoes an accelerated process of aging. In most experiments, TC procedures are performed at a relatively low number of cycles (5,000−10,000 cycles); 10,000 cycles are generally considered as 1−year equivalence, a relatively short period.[23,24] However, the longevity of RBCs in the oral cavity has been reported to be 5−22 years (average 7.8 years), making it necessary to conduct longer−frequency TC tests (i.e., with more cycles).[25,26]

The objective of this study was to evaluate the effects of long−term aging in an acidic beverage on the flexural strength (FS) and chemical structure of two different RBCs and a giomer. The FS of two RBCs and a giomer was tested using a universal testing machine following various lengths of TC (up to 100,000 cycles) in two beverages with different pHs (distilled water [DW], pH 7.0 and Coca−Cola, pH 2.4−2.8). Causative factors such as surface defects were investigated using scanning electron microscopy (SEM). To investigate the chemical changes, Filtek Z250 (3M ESPE, St. Paul, MN, USA) were analyzed as a representative RBC using Fourier transform infrared spectroscopy in attenuated total reflectance mode (FTIR−ATR) and X−ray photoelectron spectroscopy (XPS). The null hypothesis tested was that the FS and chemical structure of the RBCs would not be affected after varied frequencies of TC in two aging solutions.

MATERIALS AND METHODS

Three materials were selected to observe the difference between Conventional composite resin, Bulk fill composite resin and Giomer. The three materials have different composition of matrix and filler. The dental RBCs used in this study were Tetric N-Ceram Bulk Fill Shade A3 (Ivoclar Vivadent, Schaan, Liechtenstein) for Bulk fill RBC and Filtek Z250 microhybrid Shade A3 (3M ESPE, St. Paul, MN, USA) for Conventional RBC. A giomer, Beautifil II Shade A3 (Shofu Dental Corporation, Osaka, Japan), was also used for comparison.

The composition of the materials is shown in **Table 1**.

Sample preparation

The specimen bars for FS test were prepared using a polyethylene mold (2 mm wide × 2 mm high × 25 mm long). All composite specimens (n=420) were light-cured for 20 seconds with two parallel-bound light-guide tips of two light-emitting diode (LED) curing units (B&Lite, B&L Biotech., Gyeonggi-do, Korea). The bound tips were mounted on a stable custom-made stand and placed on the specimen in the mold. The specimen was light-cured through a 0.5 mm thick glass cover slip located in-between the specimen and light-guide tip. Each light-guide had a convex lens, which enabled two parallel-bound tips to light-cure the whole specimen at a time (Figure 1). The light intensity of the curing-light was 650 mW/cm^2, which was confirmed with a radiometer (Model 100, Kerr Demetron, Bracknell, GB) before starting the experiments and re-measured after every 20 polymerizations. When the battery power of the light curing unit decreased to 50%, the light curing unit was replaced with a fully charged one. After light curing, the samples were removed from the mold and polished with 600 grit SiC papers under copious tap water. Then, they were stored in DW at 37 ℃ for 24 hours to ensure post-cure polymerization. From the 140 specimens of each restorative, 20 specimens were randomly separated to measure the immediate FS. The remaining 120 specimens were divided into two groups: one group was placed in distilled water (DW; neutral pH) and the second group was placed in Coca-Cola (pH, 2.4-2.8; Coca-Cola, The Coca-Cola Co., Atlanta, GA, USA). Sixty specimens in each group were also divided into three subgroups (n=20 each) according to TC frequency (10,000, 50,000, and 100,000 cycles). The specimens were placed in a metal basket and thermocycled between baths containing either DW or Coca-Cola at 5 ℃and 55 ℃with a dwell time of 24 seconds and a rest time of 6 seconds. The Coca-Cola solution was changed every 3 days, and its pH was maintained between 2.48 and 2.14 using a pH meter (HI8314, Hanna instruments, Woonsocket, RI, USA). The pH of Coca-Cola in the baths was maintained lower than 2.48, even on the third day, after the evaporation of carbon dioxide gas.

FS testing

The specimens were subjected to a 4-point bending test. The sample was placed centrally on 2 lower supporting pins that were 20 mm apart. The upper loading plunger had 2 loading pins 10 mm apart, which were placed centrally over the sample. A compressive load was applied using a universal testing machine (LF Plus, Lloyd Instruments, Fareham, UK) at a crosshead speed of 0.5 mm/min until the specimen was broken.

SEM analysis

To investigate the effect of thermocycling on the surface degradation of resin composites under neutral and acidic conditions, SEM (Apreo S, Thermo Fisher Scientific, Waltham, MA, USA) was used to observe the edge adjacent to the fracture margin on the bottom surface under tension and the fractured surface of the specimen bars. After Coca-cola removal in an ultrasonic bath with warm DW for 10 seconds, the specimens were fully dried overnight in a vacuum jar, sputter-coated with platinum, and observed under SEM. The SEM images were taken at ×10,000 magnification.

FTIR-ATR analysis

FTIR-ATR spectra were recorded for Z250 only using an FTIR system (Spectrum 100, PerkinElmer, Waltham, MA, USA) equipped with an ATR unit. The ATR absorption spectra of the fully dried composite specimens were obtained from the bottom surfaces of the specimens in the region of 400–4,000 cm^{-1} wavelength using a mode of 4 scans at a resolution of 16 cm^{-1}. The absorption spectra of each cured specimen were measured four times during the study: at 4 time points of TC, i.e., after 24 hours of storage in DW (i.e., before TC), and after 10,000, 50,000, 100,000 cycles of TC in either DW or Coca-Cola. The changes in spectra after TC were analyzed according to the solution.

XPS analysis

XPS analysis (K-Alpha+, ThermoFisher Scientific, Waltham, MA, USA) was performed to compare the changes in the chemical characteristics of the bottom surface of the Z250 specimens under tension between neutral DW and acidic Coca-Cola. The measurements were carried out using an Al Ka X-ray source (1486.6 eV) at 15 kV and 100 W. The baseline pressure of the analysis chamber was maintained at approximately 2×10^{-9} mbar. The spectra of XPS were collected in a high-resolution mode with a pass energy of 40 eV and an energy step size of 0.1 eV. The energy scale was calibrated using the C1s level of 284.6 eV. The XPS spectra were processed with Shirley background subtraction and fitted with mixed Gaussian–Lorentzian functions.

Statistical analysis

SPSS version 12.0.1 (SPSS Inc, Chicago, IL, USA) was used to analyze the data obtained. The normality of the data distribution was tested using the Shapiro–Wilk test ($p>0.05$), and then parametric data analysis was used. Homogeneity of variance was assessed using the Levene test ($p>0.05$). According to 3–way analysis of variance (ANOVA), the FS values within each variable were significantly different among groups ($p<0.05$, the main effects in Table 2). There were significant interaction effects between variables ($p<0.05$), except for solution × material ($p=0.518$, Table 2). Therefore, for comparisons of variables showing significant interaction effects (i.e., material and TC), one–way ANOVA followed by the Tukey post hoc test was used for multiple comparisons. Inter–solution differences were evaluated using the t–test. All statistical analyses were carried out at a significance level of $\alpha=0.05$.

Results

Flexural strength

Before TC, similar FS results were observed for Beautifil II (giomer) and Tetric N−Ceram Bulk fill (68.57±11.73 and 69.62±7.92 MPa, respectively). In DW, there was no significant decrease in the FS at 10,000 cycles, but significant decreases were observed at 50,000 cycles in both products ($p<0.05$, Table 2). Thereafter, the FS of both restoratives did not show a significant increase or decrease at 100,000 cycles. When analyzing the Z250 specimens, the initial FS was higher than those of the other RBC and giomer, but it decreased significantly at 10,000 cycles in DW ($p<0.05$, Table 2), and it continued to decrease until 50,000 cycles ($p<0.05$). However, in Coca−Cola, the FS of both RBCs and giomer decreased rapidly at 10,000 cycles ($p<0.05$, Table 2), but thereafter, until 100,000 cycles, the FS of Beautifil II and Tetric N−Ceram did not show any statistically significant changes. However, Z250 showed an increased FS at 100,000 cycles in both aging solutions ($p<0.05$).

The FS of both RBCs and giomer was significantly lower in Coca−Cola than in DW only at 10,000 cycles (t−test, $p<0.05$). At 50,000 and 100,000 cycles, the FS of each restorative became statistically equivalent in both aging solutions.

SEM analysis

In initial samples, fillers with various sizes and shapes were observed, and small pores were observed between fillers (Figures 2-0, 3-0, and 4-0). As the number of cycles increased, irregularly-shaped larger fillers and more pores were observed on the surfaces of the specimens. For the same number of cycles, more pores were observed in Coca-Cola than in DW. In the condition of 10,000 cycles in DW, fillers on the surface were observed (Figures 2-a, 3-a, and 4-a), but in the Coca-Cola solution, fillers were not observed on the surface; instead, the resin matrix with scattered small pores covered on the specimen surface (Figures 2-A, 3-A, and 4-A). In DW, small pores became increasingly prevalent at 50,000 cycles, and defects where the fillers were peeled off were observed as surface pores at 100,000 cycles; however, many filler particles were still observed (Figures 2-c, 3-c, and 4-c). In Coca-Cola, at 10,000 cycles, the surface mostly consisted of resin matrix with pores containing a few filler remnants; after 50,000 cycles, the pores were increased and enlarged (Figures 2-B, 3-B, and 4-B). After 100,000 cycles in Coca-Cola, the cavities where the fillers were peeled off were connected, leaving behind large defects and narrow matrix networks (Figures 2-C, 3-C, and 4-C).

The three restorative materials showed different features on SEM. Beautifil II had irregularly shaped fillers of various sizes and numerous small pores (Figure 2-0). Compared to Beautifil II, the pores of Tetric-N-Ceram were clearly smaller (Figure 3-0). In the case of Z250, irregularly shaped larger nanocluster fillers and small round fillers were initially observed on the specimen surface (Figure 4-0). The small pores increased from 10,000 to 100,000 cycles, but were present to a much lesser extent than in Beautifil II and Tetric-N-Ceram. After 100,000 cycles in Coca-Cola, large holes caused by peeled-off fillers were also observed in the samples (Figure 4-C).

FTIR-ATR analysis

Peaks originating from functional groups of the base resin, including bis-GMA, TEGMDA and urethane dimethacrylate (UDMA), and fillers were observed in the FTIR-ATR spectra of Z250. The aliphatic C=C peak at 1638 cm^{-1} decreased after polymerization, confirming that polymerization took place (Figures 5 and 6). In DW, no differences were found in the shape and position of the ester peak (R−COO−R) at 1718 cm^{-1} or the hydroxyl peak (−OH) at 3340 cm^{-1} according to increasing number of cycles (Figure 5). However, when specimens were treated in Coca−Cola, the shape and position of hydroxyl peak were broadened and shifted to 3270 cm^{-1} (Figure 6, from narrow red peak to broad green peak in the left box). These hydroxyl peaks must have originated from the −OH group in the matrix and added by the hydrolysis reaction. Another broad peak corresponding to the ester group in the matrix resin was observed between 1730 cm^{-1} and 1700 cm^{-1} in the FTIR−ATR spectra of the unaged specimens and specimens aged in DW, while a sharp peak corresponding to the ester groups left at 1733 cm^{-1} in the spectra of specimens aged in Coca−Cola (Figure 6, from broad red peak to narrow green peak in the right box).

XPS analysis

The atomic compositions and chemical characteristics of Z250 were characterized by XPS analysis. Peaks corresponding to C, O, F, Al, Si, Zr, Ba, and Yb were observed in the XPS wide−scan spectra of the composite. As shown in Figure 7, the observed C1s peak was deconvoluted into its component peaks. In Z250, the intensity of the ether peak (C−O) relative to other peaks, especially C=C peak, increased after TC (Figure 7). In DW, it was observed that the relative peak intensity of the ether group gradually increased with prolonged TC. The relative peak intensity of the ether group after 10,000 cycles in Coca−Cola was almost the same as that after 100,000 cycles in DW (Figure 7). The relative decrease of the C=C peak and the relative increase of the C−O peak resulted from the removal of the unreacted functional group, C=C, from the surface. In water, gradual elimination (wash−out) of unreacted aliphatic C=C groups occurred slowly, but this reaction occurred more easily and faster in acidic conditions (Coca−Cola, Figure 7).

The Si−O peak was relatively higher than that of Si−C after 10,000 cycles in DW, and it progressively increased until 100,000 cycles (Figure 8). In Coca−Cola, the relative intensity was not as consistent as in DW, and after 100,000 cycles, it was at the same level as in DW.

Discussion

This study investigated how the mechanical strength and chemical characteristics of RBCs and a giomer changed after long-term aging in an acidic environment. The specimens were aged for 100,000 cycles, approximating 10 years of clinical service.[23,24] Changes in the mechanical strength were evaluated by measuring the FS with a four-point bending test. The surface changes observed using SEM were used to interpret changes in the FS visually. The decrease in the FS was correlated with surface degradation in the SEM images. The chemical changes in the functional groups and the changes in the binding energy were explained using FTIR and XPS of Z250, respectively. As the main finding of this study, the FS decreased with an increasing number of cycles, but it decreased more rapidly in the acidic environment at 10,000 cycles. In the SEM images, more pores were observed in Coca-Cola than in DW. According to the FTIR-ATR analysis of Z250, an additional hydroxyl peak was added at around 3200 cm^{-1}, and the ester peak at 1700 cm^{-1} disappeared in the Coca-Cola, in contrast to what was observed in DW. In XPS, a relative increase of the C-O peak occurred gradually in DW, but rapidly in Coca-Cola.

In DW, a steady increase in the Si–O peak was observed, unlike in Coca–Cola. Therefore, the null hypothesis that the FS and the chemical structure of RBCs and a giomer would not be affected after varied frequencies of TC in two aging solutions with different pH values was rejected.

After 10,000 cycles, FS decreased significantly in Coca–Cola compared to DW. The FS values of the RBCs and the giomer in Coca–Cola after 10,000 cycles were approximately the same as those after 50,000 cycles in DW, and this finding may be an indication that TC in Coca–Cola exhibits an aging effect 5 times faster than TC in DW. After 100,000 cycles in both conditions, the FS of Z250 increased slightly but significantly, in comparison to the continuous decrease of the FS until 50,000 cycles. However, the FS of the other RBC and the giomer (Beautifil II and Tetric N–Ceram Bulk Fill) was statistically equivalent after 50,000 or 100,000 cycles. The increase in the FS of Z250 after 100,000 cycles may be a result of an increase in polymerization due to the warm temperature (55℃) during TC.[4, 27, 28] A few previous study performed TC up to 100,000 cycles, and additional research is needed to investigate the changes in the degree of conversion (DC) according to the number of cycles.

After polymerization, a dental RBC becomes brittle. Surface observations are important because the strength is affected by the distribution of cracks.[29,30] In this study, the specimen surface after four-point bend flexural strength test was observed under SEM. The SEM images clearly showed the shape of the fillers and defects that occurred after TC. In all the RBCs and giomer, defects increased as the number of cycles increased, but the surface degradation patterns were different among restorative materials. The highest porosity was observed for Beautifil II, followed in descending order by Tetric N-Ceram Bulk Fill and Filtek Z250. In Beautfil II, the surface porosity after 10,000 cycles in Coca-Cola was similar to that after 100,000 cycles in DW. In Tetric N-Ceram Bulk fill and Z250, the specimens after 10,000 cycles in DW showed relatively low porosity. The pores after 50,000 cycles and 100,000 cycles in DW appeared similar to those after 10,000 cycles and 50,000 cycles in Coca-Cola, respectively. Both RBCs showed increased porosity after 100,000 cycles in Coca-Cola, but to a lesser extent than observed in Beautifil II after 10,000 cycles. Beautifil II showed significantly more porosity than the other RBCs after 100,000 cycles in DW and even after 10,000 cycles in Coca-Cola. An explanation for this might relate to differences in fillers and matrix monomers, including their composition, size, and processing methods.[31,32,33]

Beautifil II has a specific filler system that contains S−PRG fillers. S−PRG fillers are basically fluoroaluminosilicate glasses, which are pre−reacted with polyacrylic acid and then milled into irregularly square filler particles of 1 μm in size, with few interdispersed round filler particles of 20−50 nm in size, after which it is treated with silane. Therefore, after TC in DW, the fillers of Beautifil II showed distinctive filler boundaries and shapes and dehydration cracks, which were characteristic of glass ionomer cements and more pronounced after TC in Coca−Cola. The findings in this study are consistent with the descriptions in previous reports.[34,35,36] The large number of holes on the surfaces of the Beautifil II specimens were also described in the previous report,[37] in which they were attributed to dissolution of the S−PRG filler particles in acidic conditions. In addition, the microstructural pores and voids were also attributed to differences in the shrinkage rates between fillers and matrix and loose bonding of glass filler particles to the matrix. Beautifil II has a higher percentage of TEGDMA as a constituent. Compared to other matrix monomers, TEGDMA has a lower molecular weight and is more hydrophilic, so it is easy to hydrolyze.[38,39] Therefore, it seems that hydrolysis of Beautifil II is easier than other RBCs, showing extensive porosity. In Beautifil II, a spherical S-PRG filler was clearly observed, and in Tetric N-Ceram and Z250, an irregular polygonal filler was observed. Some of the fillers of Z250 were observed in the form of large lumps, unlike Tetric N-Ceram Bulk Fill. The silane treatment method may be different for each manufacturer, and this method is not disclosed.

In the SEM images, more porosity was observed in Coca-Cola than in DW, and it was considered that FS decreased because there were more defects on the surface—that is, there was an increased distribution of cracks. However, Beautifil II showed the most porosity after 100,000 cycles in Coca-Cola, but the FS value did not decrease significantly. Only the surface may be damaged and the inside of specimen may have still been intact; this is a limitation of the methodology of analyzing surface degradation.

In the FTIR-ATR spectra of the Z250 specimens aged in Coca-Cola, the broad ester peak (1730-1700 cm^{-1} peak; red peak in the right box of Figure 6; red peak of the right illustrations in Figure 9) observed in DW changed, and only a sharp peak (1733 cm^{-1}; green peak in the right box of Figure 6; green peak of the right illustrations in Figure 9) remained. A broad peak was formed by combining the peaks for the α,β-unsaturated ester (1730-1715

cm^{-1}; orange peak of the right-middle illustration in Figure 9) bonded to the unreacted C=C group and the ester (1750-1735 cm^{-1}; green peak of the right-middle illustration in Figure 9) present in the polymer. When α,β-unsaturated ester was hydrolyzed in an acidic environment, an -OH group left at the end of the polymer (blue OH group in Figure 9) but methacrylic acid (MA; orange portion in Figure 9) was removed from the matrix. Therefore, only the sharp peak at 1733 cm^{-1} from the ester remaining in the polymer after TC was observed in the specimens aged in Coca-Cola. The -OH peak observed at 3340 cm^{-1} (red peak in the left box of Figure 6; red peak in the left illustrations in Figure 9) is an alcohol present in Bis-GMA, which is shared by these RBCs and giomer. Hydrolysis of the ester under acidic conditions formed a new -OH group, which was not previously observed. The peak of this new -OH group (blue peak of the left illustrations in Figure 9) merged with the existing -OH peak (red peak of the left illustrations in Figure 9), broadening the OH peak and shifting the center of the OH peak from 3340 cm^{-1} to 3270 cm^{-1} (green peak in the left box of Figure 6 and green peak of the left illustrations in Figure 9). In case of Z250 in Coca-Cola, the peak changed after 10,000 cycles, but in DW, there was no change even after 100,000 cycles. This means that hydrolysis of the resin matrix can be accelerated in an acidic environment. Therefore, it might be suggested that the resin matrix of commercial RBCs and giomers can be hydrolyzed easily in acidic conditions such as drinking coffee and Coke. Also, if the pH of saliva drops below 7 after meal, saliva may cause hydrolysis of the resin matrix. In addition to the dissolution and/or exfoliation of filler particles, the degradation of the resin matrix might have also contributed to the decrease in the FS of the RBCs and giomer, as confirmed by the larger pores and shrunken resin matrix networks in the specimens after longer TC durations (e.g.,50,000 or 100,000 cycles) in Coca-Cola.

A peak from a functional group may be composed of multiple peaks with different binding energies. Changing the composition of a functional group with different binding energies can shift the shape of the peak.[40,41] Changes in the peaks of ester and hydroxyl groups were observed in Coca-Cola. During TC at 55° C, the large amount of H^+ contained in Coca-Cola can hydrolyze Bis-GMA into bishydroxy-propoxy-phenyl-propane (Bis-HPPP) and MA (orange portion in Figure 9). Bis-HPPP gained an additional -OH group (blue portion in Figure 9). As a result of hydrolysis in Coca-Cola, a carboxylic acid, MA (orange portion in Figure 9) was washed out and removed from the surface, which narrowed and shifted the ester peak from between 1730 cm^{-1} and 1700 cm^{-1} to 1733 cm^{-1} (from red to green in the right illustrations of Figures 6 and 9). In contrast, the other end of hydrolyzed Bis-GMA (Bis-HPPP) changes to an -OH group (blue portion in Figure 9) and it adds another OH peak to the spectrum and makes the peak shift and broaden; thus, the peak shifts from 3340 cm^{-1} to 3270 cm^{-1} (from red to green in the left illustrations of Figures 6 and 9). It can be inferred that the ester and hydroxyl groups included in the RBCs and giomer were affected by hydrolysis, which was accelerated by the acidic conditions in the Coca-Cola aging solution.

An attempt was made to measure the DC from the FTIR-ATR spectra. Although the two parallel-bound light-guide tips (10 mm each) did not cover the entire surface of the mold, the whole specimen (25 mm) was completely polymerized because they had convex lenses. At least, they covered the whole length between two supporting pins (20 mm). Even with the convex lenses, the light intensity of each light-guide tip was confirmed over 650 mW/cm^{-2} with a radiometer. The even polymerization of the whole specimen was confirmed by observing that the fractures were happened near the center of the specimen, at least between the two plunger pins (10 mm). In addition, the DC obtained using FTIR-ATR showed relevant values within a reliable range in each group and condition. The specimens aged in DW showed DC values of 60%–70%, but those in Coca–Cola showed DC values of 30%–40%. Because of the degradation of the resin matrix by long–term aging in acidic conditions, as described in the previous paragraph, some of the aliphatic C=C double bonds might have been lost. When Bis–GMA is hydrolyzed in acidic conditions, MA is cleaved from the matrix and washed out, which may remove some of the aliphatic C=C double bonds. To obtain the DC, the peaks of aromatic double bonds at 1608 cm^{-1} and the aliphatic double bonds at 1638 cm^{-1} are used. As the 1733 cm^{-1} peak changed in Coke, the 1638–1608 cm^{-1} part also changed. Therefore, it was difficult to measure the DC consistently after long–term hydrolysis of the resin matrix, so the DC data was not included in this report. When measuring the DC of aged specimens, it should be considered that the C=C double bonds cleaved from matrix polymer may be washed out, in addition to the change to single bonds by polymerization.

As shown on the XPS spectra, when the number of cycles increased, the intensity of the C1s (C=C) peak decreased relatively compared to that of the C1s (C–O) peak in both aging conditions (Figure 7). The C=C bond exists as a functional group at the end of the matrix monomer and at the end of the silane (γ−MPS), while the C−O bond exists in the middle of the matrix monomer. The C=C peak might be decreased as a result of the hydrolysis of unreacted monomers and subsequent washing−out. In contrast, the C−O bond present in the middle of the polymer was not affected after TC, compared to the C=C bond which was washed−out by hydrolysis during TC; resulting in a relatively high C−O peak. In the DW conditions, the intensity of the C−O peak relative to that of C=C peak gradually increased with the number of cycles (Figure 7, upper row); however, in Coca−Cola conditions, that of the C−O bond increased rapidly (Figure 7, lower row). An explanation for this is that the relative intensity of the C=C peak rapidly decreased due to hydrolysis and subsequent wash−out. The change of the peak after 10,000 cycles in Coca−Cola was more rapid than the change of the peak after 100,000 cycles in DW. This suggests that a stronger chemical reaction occurs when TC is performed in Coca−Cola, which may result in rapid degradation at the filler−resin matrix interface and even within the resin matrix. In addition, the change in the ester peak after 10,000 cycles in Coca−Cola, which was observed in the FTIR−ATR spectra, explains the rapid increase in the C−O peak after 10,000 cycles of XPS. The change in the ester peak of FTIR−ATR means that the MA was washed out. Since MA included C=C, when MA was removed from the surface, XPS showed a relative increase in C−O. The results of XPS for the C=C and C−O peaks are consistent with the SEM observations and FTIR analyses regarding the finding that the FS decreased rapidly after 10,000 cycles in Coca−Cola, whereas it decreased gradually in DW.

Inconsistency was observed in the relative intensity of C−O peak compared to C=C peak after 100,000 TC in Coca−Cola. Unlike the intensity of C−O peak in DW showing a gradual increase up to 100,000 TC (Figure 7, upper row), the intensity of C−O peak was rapidly increased after 10,000 TC in Coca−Cola and continued until after 50,000 TC; but it was decreased after 100,000 TC in Coca−Cola (Figure 7, lower row); nevertheless, it was still high about at the level after 100,000 TC in DW. Additional research needs to be performed to understand why the relative intensity of C−O peak did not increase continuously. This may be related to the slight increase of FS after 100,000 TC.

The bonding between silica and γ−MPS, which is called silanization, mediates the bonding between the inorganic filler and the organic matrix (Figure 10). The Si−C bond is only observed in silane coupling agent, and a decrease in the Si−C peak directly indicates the removal of silane coupling agent from the surface. The

Si-O bond is observed in both silica and silane coupling agent; thus, a decrease in the ratio of Si-C/Si-O might be caused by washing-out of silane coupling agent.[42] Regarding the ratio of the Si-C and Si-O peaks, the Si-O peak was higher in DW than in Coca-Cola. In DW, as the matrix and unpolymerized silane were removed from the surface, silica was exposed and the Si-O peak continuously increased (Figure 8, upper row). In contrast, in Coca-Cola, a possible explanation for the pronounced decrease in the ratio of Si-C/Si-O is that the silane and fillers might have been separated together with the destruction of the matrix (Figure 8, lower row).

This study measured the changes in the FS and chemical properties of two RBCs and a giomer after long-term aging and investigated the interaction between RBCs/giomer and acidic beverages using Coca-Cola as an example. Long-term TC in Coca-Cola can cause hydrolysis on the surface of two RBCs and a giomer, demonstrating the potential for hydrolysis of the matrix and exfoliation of fillers.

Conclusion

In DW, the matrix of RBCs is less likely to be affected by hydrolysis, but unreacted monomers and silane are washed out by hydrolysis, resulting in gradual changes in porosity and FS. In contrast, chemical changes occurred rapidly in an acidic environment and destroyed the matrix. As a result. The hydrolysis of the matrix in Coca-Cola caused rapid surface degradation, reduction of FS, and large pores.

References

1. Ferracane, J. L. (2011). Resin composite—state of the art. *Dental Materials*, *27*(1), 29-38. https://doi.org/10.1016/j.dental.2010.10.020
2. Villarroel, M., Fahl, N., De Sousa, A. M., & de Oliveira, O. B. (2011). Direct esthetic restorations based on translucency and opacity of composite resins. *Journal of Esthetic and Restorative Dentistry*, *23*(2), 73-87. https://doi.org/10.1111/j.1708-8240.2010.00392.x
3. Elekdag-Turk, S., Turk, T., Isci, D., & Ozkalayci, N. (2008). Thermocycling effects on shear bond strength of a self-etching primer. *The Angle Orthodontist*, *78*(2), 351-356. https://doi.org/10.2319/122906-537.1

4. Ghavami-Lahiji, M., Firouzmanesh, M., Bagheri, H., Kashi, T. S. J., Razazpour, F., & Behroozibakhsh, M. (2018). The effect of thermocycling on the degree of conversion and mechanical properties of a microhybrid dental resin composite. *Restorative Dentistry & Endodontics*, *43*(2). https://doi.org/10.5395/rde.2018.43.e26

5. Cilli, R., Pereira, J. C., & Prakki, A. (2012). Properties of dental resins submitted to pH catalysed hydrolysis. *Journal of Dentistry*, *40*(12), 1144-1150. https://doi.org/10.1016/j.jdent.2012.09.012

6. Lee, C., Kashima, K., Ichikawa, A., Yamaguchi, S., & Imazato, S. (2020). Influence of hydrolysis degradation of silane coupling agents on mechanical performance of CAD/CAM resin composites: In silico multi-scale analysis. *Dental Materials Journal*, *39(5)* 2019-223. https://doi.org/10.4012/dmj.2019-223

7. Monticelli, F., Osorio, R., Toledano, M., Tay, F. R., & Ferrari, M. (2006). In vitro hydrolytic degradation of composite quartz fiber-post bonds created by hydrophilic silane couplings. *Operative Dentistry*, *31*(6), 728-733.https://doi.org/10.2341/05-151

8. Szczesio-Wlodarczyk, A., Sokolowski, J., Kleczewska, J., & Bociong, K. (2020). Ageing of dental composites based on

methacrylate resins—A critical review of the causes and method of assessment. *Polymers*, *12*(4), 882. https://doi.org/10.3390/polym12040882

9. Rusnac, M. E., Gasparik, C., Irimie, A. I., Grecu, A. G., Mesaroş, A. Ş., & Dudea, D. (2019). Giomers in dentistry–at the boundary between dental composites and glass−ionomers. *Medicine and Pharmacy Reports*, *92*(2), 123. https://doi.org/10.15386/mpr−1169
10. Quader, S. A., Alam, M. S., Bashar, A. K. M., Gafur, A., & Al Mansur, M. A. (2012). Compressive strength, fluoride release and recharge of giomer. *Update Dental College Journal*, *2*(2), 28−37. https://doi.org/10.3329/updcj.v2i2.15533
11. Fujimoto, Y., Iwasa, M., Murayama, R., Miyazaki, M., Nagafuji, A., & Nakatsuka, T. (2010). Detection of ions released from S−PRG fillers and their modulation effect. *Dental Materials Journal*, 29(4) 392−397.https://doi.org/10.4012/dmj.2010−015
12. Shimazu, K., Ogata, K., & Karibe, H. (2011). Evaluation of the ion−releasing and recharging abilities of a resin−based fissure sealant containing S−PRG filler. *Dental Materials Journal*, 30(6), 923−927. https://doi.org/10.4012/dmj.2011−124
13. Veloso, S. R. M., Lemos, C. A. A., de Moraes, S. L. D., do Egito

Vasconcelos, B. C., Pellizzer, E. P., & de Melo Monteiro, G. Q. (2019). Clinical performance of bulk−fill and conventional resin composite restorations in posterior teeth: a systematic review and meta−analysis. *Clinical Oral Investigations*, *23*(1), 221−233. https://doi.org/10.1007/s00784−018−2429−7

14. Ilie, N., Bucuta, S., & Draenert, M. (2013). Bulk−fill resin−based composites: an in vitro assessment of their mechanical performance. *Operative Dentistry*, *38*(6), 618−625. https://doi.org/10.2341/12−395−L
15. Ehlen, L. A., Marshall, T. A., Qian, F., Wefel, J. S., & Warren, J. J. (2008). Acidic beverages increase the risk of in vitro tooth erosion. *Nutrition Research*, *28*(5), 299−303. https://doi.org/10.1016/j.nutres.2008.03.001
16. Korte, A., Angelopoulou, M. V., & Maroulakos, G. (2019). Assessing the effect of low calorie soda beverages on primary tooth enamel: an in vitro study. *Journal of Clinical Pediatric Dentistry*, *43*(3), 190−195. https://doi.org/10.17796/1053−4625−43.3.8
17. Ehlen, L. A., Marshall, T. A., Qian, F., Wefel, J. S., & Warren, J. J. (2008). Acidic beverages increase the risk of in vitro tooth erosion. *Nutrition Research*, *28*(5), 299−303.

https://doi.org/10.1016/j.nutres.2008.03.001

18. Low, I. M., & Alhuthali, A. (2008). In−situ monitoring of dental erosion in tooth enamel when exposed to soft drinks. *Materials Science and Engineering: C*, *28*(8), 1322−1325 https://doi.org/10.1016/j.msec.2008.02.005
19. Eweis, A. H., Yap, A. U., & Yahya, N. A. (2020). Comparison of flexural properties of bulk−fill restorative/flowable composites and their conventional counterparts. *Operative Dentistry*, *45*(1), 41−51. https://doi.org/10.2341/18−133−L
20. Özel Bektas, Ö., Eren, D., Herguner Siso, S., & Akin, G. E. (2012). Effect of thermocycling on the bond strength of composite resin to bur and laser treated composite resin. *Lasers in Medical Science*, *27*(4), 723−728. https://doi.org/10.1007/s10103−011−0958−2
21. Camilotti, V., Mendonça, M. J., Dobrovolski, M., Detogni, A. C., Ambrosano, G. M., & Mario F, D. G. (2021). Impact of dietary acids on the surface roughness and morphology of composite resins. *Journal of Oral Science*, *63*(1), 18−21. https://doi.org/10.2334/josnusd.19−0518.
22. Badra, V. V., Faraoni, J. J., Ramos, R. P., & Palma−Dibb, R. G. (2005). Influence of different beverages on the microhardness

and surface roughness of resin composites. *Operative Dentistry*, *30*(2), 213-9.

23. Tuncer, S., Demirci, M., Tiryaki, M., Ünlü, N., & Uysal, Ö. (2013). The effect of a modeling resin and thermocycling on the surface hardness, roughness, and color of different resin composites. *Journal of Esthetic and Restorative Dentistry*, *25*(6), 404-419. https://doi.org/10.1111/jerd.12063
24. Özel Bektas, Ö., Eren, D., Herguner Siso, S., & Akin, G. E. (2012). Effect of thermocycling on the bond strength of composite resin to bur and laser treated composite resin. *Lasers in Medical Science*, *27*(4), 723-728.
25. Opdam, N. J. M., Van De Sande, F. H., Bronkhorst, E., Cenci, M. S., Bottenberg, P., Pallesen, U., ... & Van Dijken, J. W. (2014). Longevity of posterior composite restorations: a systematic review and meta-analysis. *Journal of Dental Research*, *93*(10), 943-949. https://doi.org/10.1177/0022034514544217
26. Demarco, F. F., Corrêa, M. B., Cenci, M. S., Moraes, R. R., & Opdam, N. J. (2012). Longevity of posterior composite restorations: not only a matter of materials. *Dental Materials*, *28*(1), 87-101. https://doi.org/10.1016/j.dental.2011.09.003

27. Pereira, J. R., Júnior, L. C., & Júnior, N. F. (2017). Effect of thermocycling and varying polymerization techniques on the restorative interface of class V cavities restored with different composite resin systems. *Journal of Clinical and Experimental Dentistry*, *9*(3), e405. http://dx.doi.org/10.4317/jced.53481

28. Oliveira, J. C. D., Aiello, G., Mendes, B., Urban, V. M., Campanha, N. H., & Jorge, J. H. (2010). Effect of storage in water and thermocycling on hardness and roughness of resin materials for temporary restorations. *Materials Research*, *13*, 355–359. https://doi.org/10.1590/S1516-14392010000300013

29. Shah, M. B., Ferracane, J. L., & Kruzic, J. J. (2009). Mechanistic aspects of fatigue crack growth behavior in resin based dental restorative composites. *Dental Materials*, *25*(7), 909–916. https://doi.org/10.1016/j.dental.2009.01.097

30. Toparli, M., & Aksoy, T. (1998). Fracture toughness determination of composite resin and dentin/composite resin adhesive interfaces by laboratory testing and finite element models. *Dental Materials*, *14*(4), 287–293. https://doi.org/10.1016/S0109-5641(98)00041-4

31. Lung, C. Y. K., Sarfraz, Z., Habib, A., Khan, A. S., & Matinlinna, J. P. (2016). Effect of silanization of hydroxyapatite fillers on

physical and mechanical properties of a bis−GMA based resin composite. *Journal of the Mechanical Behavior of Biomedical Materials*, *54*, 283−294. https://doi.org/10.1016/j.jmbbm.2015.09.033

32. MUNKSGAARD, E. C., & FREUND, M. (1990). Enzymatic hydrolysis of (di) methacrylates and their polymers. *European Journal of Oral Sciences*, *98*(3), 261−267. https://doi.org/10.1111/j.1600−0722.1990.tb00971.x

33. Söderholm, K. J., Zigan, M., Ragan, M., Fischlschweiger, W., & Bergman, M. (1984). Hydrolytic degradation of dental composites. *Journal of Dental Research*, *63*(10), 1248−1254. https://doi.org/10.1177/00220345840630101701

34. Yap, A. U. J., Tan, S. H. L., Wee, S. S. C., Lee, C. W., Lim, E. L. C., & Zeng, K. Y. (2001). Chemical degradation of composite restoratives. *Journal of Oral Rehabilitation*, *28*(11), 1015−1021. https://doi.org/10.1111/j.1365−2842.2001.00760.x

35. An, J., Park, H., Seo, H., & Lee, S. (2015). Antibacterial properties of pit and fissure sealant containing S−PRG filler on Streptococcus mutans. *Journal of the Korean Academy of Pedtatric Dentistry*, *42*(4), 302−311. https://doi.org/10.5933/JKAPD.2015.42.4.302

36. Mayumi, K., Miyaji, H., Miyata, S., Nishida, E., Furihata, T., Kanemoto, Y., ... & Akasaka, T. (2021). Antibacterial coating of tooth surface with ion-releasing pre-reacted glass-ionomer (S-PRG) nanofillers. *Heliyon*, *7*(2), e06147. https://doi.org/10.1016/j.heliyon.2021.e06147

37. Yoshihara, K., Nagaoka, N., Maruo, Y., Sano, H., Yoshida, Y., & Van Meerbeek, B. (2017). Bacterial adhesion not inhibited by ion-releasing bioactive glass filler. *Dental Materials*, *33*(6), 723-734. https://doi.org/10.1016/j.dental.2017.04.002

38. IMAZATO, S., TARUMI, H., KATO, S., EBI, N., EHARA, A., & EBISU, S. (1999). Water sorption, degree of conversion, and hydrophobicity of resins containing Bis-GMA and TEGDMA. *Dental Materials Journal*, *18*(1), 124-132. https://doi.org/10.4012/dmj.18.124

39. Geurtsen, W., & Leyhausen, G. (2001). Concise review biomaterials & bioengineering: chemical-biological interactions of the resin monomer triethyleneglycol-dimethacrylate (TEGDMA). *Journal of Dental Research*, *80*(12), 2046-2050. https://doi.org/10.1177/00220345010800120401

40. Martinez-Felipe, A., Cook, A. G., Abberley, J. P., Walker, R., Storey, J. M., & Imrie, C. T. (2016). An FT-IR spectroscopic

study of the role of hydrogen bonding in the formation of liquid crystallinity for mixtures containing bipyridines and 4-pentoxybenzoic acid. *Rsc Advances*, *6*(110), 108164–108179. https://doi.org/10.1039/C6RA17819G

41. Yuan, L., Wan, J., Ma, Y., Wang, Y., Huang, M., & Chen, Y. (2013). The content of different hydrogen bond models and crystal structure of eucalyptus fibers during beating. *BioResources*, *8*(1), 717–734. https://doi.org/10.15376/biores.8.1.717-734

42. Monticelli, F., Osorio, R., Toledano, M., Tay, F. R., & Ferrari, M. (2006). In vitro hydrolytic degradation of composite quartz fiber-post bonds created by hydrophilic silane couplings. *Operative Dentistry*, *31*(6), 728–733. https://doi.org/10.2341/05-151

Table1. Composition of dental composite resins used in this study

Product name (Abbreviation)	Type	Organic matrix (Photoinitiator)	Filler	Filler content (wt%)
Beautifil II (Shofu, Osaka, Japan)(B)	Giomer	Bis-GMA TEGDMA (CQ)	S-PRG filler, multifunctional glass filler	83.3 wt% (68.6 vol%)
Tetric N-Ceram Bulk Fill (Ivoclar Vivadent,Schaan, Liechtenstein)(T)	Bulk-fill restorative composite	Bis-GMA Bis-EMA UDMA (CQ, TPO, Ivocerin)	barium glass, ytterbium trifluoride, mixed oxide, prepolymer	75-77% (53-55 vol%)
Filtek Z250 (3M ESPE, St. Paul, MN, USA)(Z)	Microhybird composite	Bis-EMA, UDMA Bis-GMA TEGDMA (CQ)	zirconia/silica	78% (60 vol%)

Abbreviations: Bis-GMA, bisphenol A diglycidyl ether dimethacrylate; Bis-EMA, bis-phenol A polyethylene glycol diether dimethacrylate; CQ, camphorquinone; TEGDMA, triethyleneglycol-dimethacrylate; TPO, 2,4,6-trimethylbenzoyl diphenylphosphine oxide; S-PRG, surface pre-reacted glass ionomer; UDMA, urethane dimethacrylate.

Table 2. Changes of the flexural strength of two resin−based composite resins and a giomer according to increasing thermo−cyclings and different aging solutions

Flexural strength (n = 20, MPa)

Material	Thermocycling	Aging solution		Results of 3-way ANOVA
		DW	Coca-Cola	
Beautifil II	0 (immediate)*	68.57 ± 11.73^{Abc}	68.57 ± 11.73^{Ab}	Main effects: solution, *p*<0.05 material, *p*<0.05 TC, *p*<0.05 Interaction effects: solution × material, *p*=0.518 material × TC, *p*<0.05 TC × solution, *p*<0.05 solution × material × TC, *p*<0.05
	10,000	69.91 ± 11.17^{Abc}	45.50 ± 9.78^{Bdef}	
	50,000	48.04 ± 7.29^{Aef}	48.88 ± 6.87^{Acde}	
	100,000	51.29 ± 8.84^{Adef}	55.24 ± 6.05^{Acd}	
Tetric N-Ceram Bulk fill	0 (immediate)*	69.62 ± 7.92^{Abc}	69.62 ± 7.92^{Ab}	
	10,000	58.63 ± 11.53^{Acde}	45.34 ± 5.00^{Bef}	
	50,000	40.05 ± 6.19^{Af}	38.06 ± 4.13^{Af}	
	100,000	46.82 ± 7.21^{Aef}	44.34 ± 5.17^{Aef}	
Z250	0 (immediate)*	127.06 ± 15.01^{Aa}	127.06 ± 15.01^{Aa}	
	10,000	80.26 ± 18.67^{Ab}	66.42 ± 7.39^{Bb}	
	50,000	62.90 ± 14.09^{Acd}	55.74 ± 14.01^{Ac}	
	100,000	75.58 ± 12.62^{Ab}	68.67 ± 11.32^{Ab}	

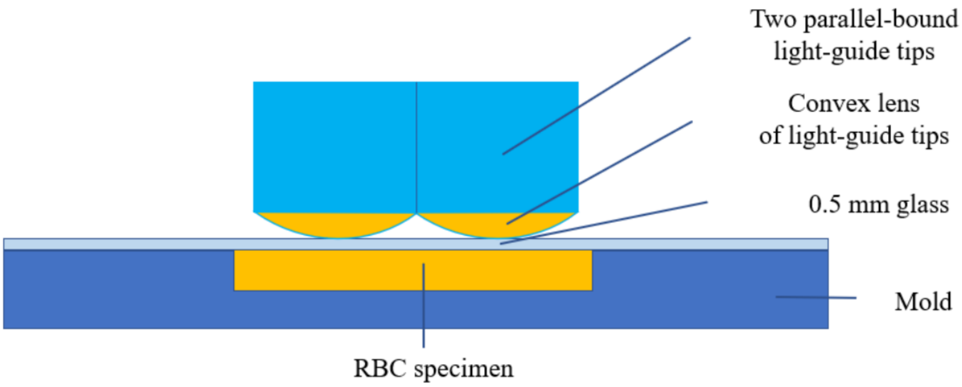

Figure 1. Schematic illustration of light-curing of samples in a polyethylene mold (2 mm wide × 2 mm high × 25 mm long).

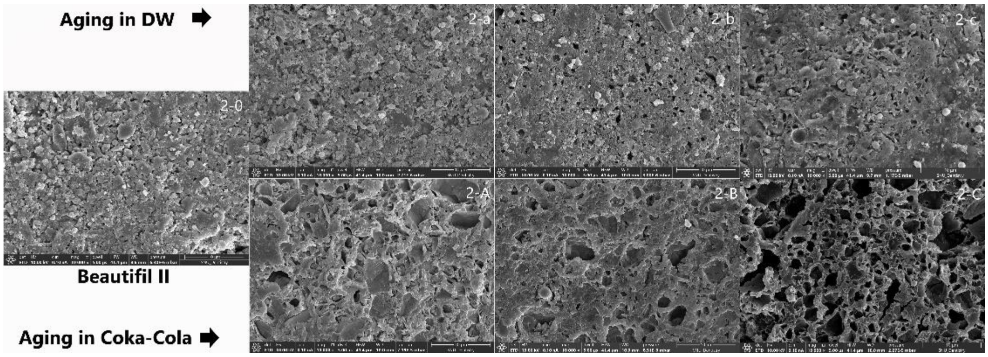

Figure 2. Changes in the scanning electron microscopic images of Beautifil II with prolonged thermocycling. After 100,000 cycles in Coca-Cola, noticeable pores are observed. a, 10,000 cycles in DW; b, 50,000 cycles in DW; c, 100,000 cycles in DW; A, 10,000 cycles in Coca-Cola; B, 50,000 cycles in Coca-Cola; C, 100,000 cycles in Coca-Cola. DW, distilled water.

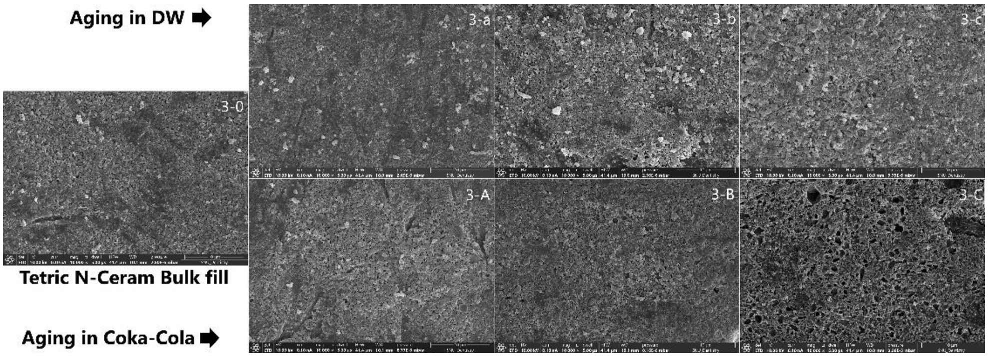

Figure 3. Changes in the scanning electron microscopic images of Tetric N−Ceram Bulk fill with prolonged thermocycling. After 100,000 cycles in Coca−Cola, noticeable pores are observed. a, 10,000 cycles in DW; b, 50,000 cycles in DW; c, 100,000 cycles in DW; A, 10,000 cycles in Coca−Cola; B, 50,000 cycles in Coca−Cola; C, 100,000 cycles in Coca−Cola. DW, distilled water.

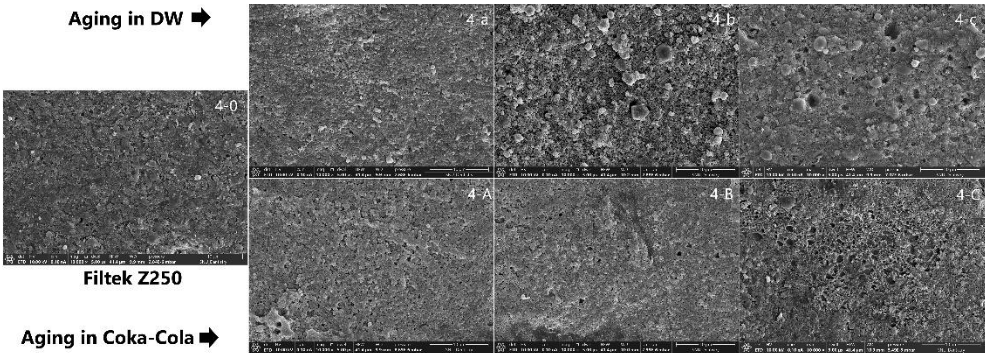

Figure 4. Changes in the scanning electron microscopic images of Z250 with prolonged thermocycling. a, 10,000 cycles in DW; b, 50,000 cycles in DW; c, 100,000 cycles in DW; A, 10,000 cycles in Coca-Cola; B, 50,000 cycles in Coca-Cola; C, 100,000 cycles in Coca-Cola. DW, distilled water.

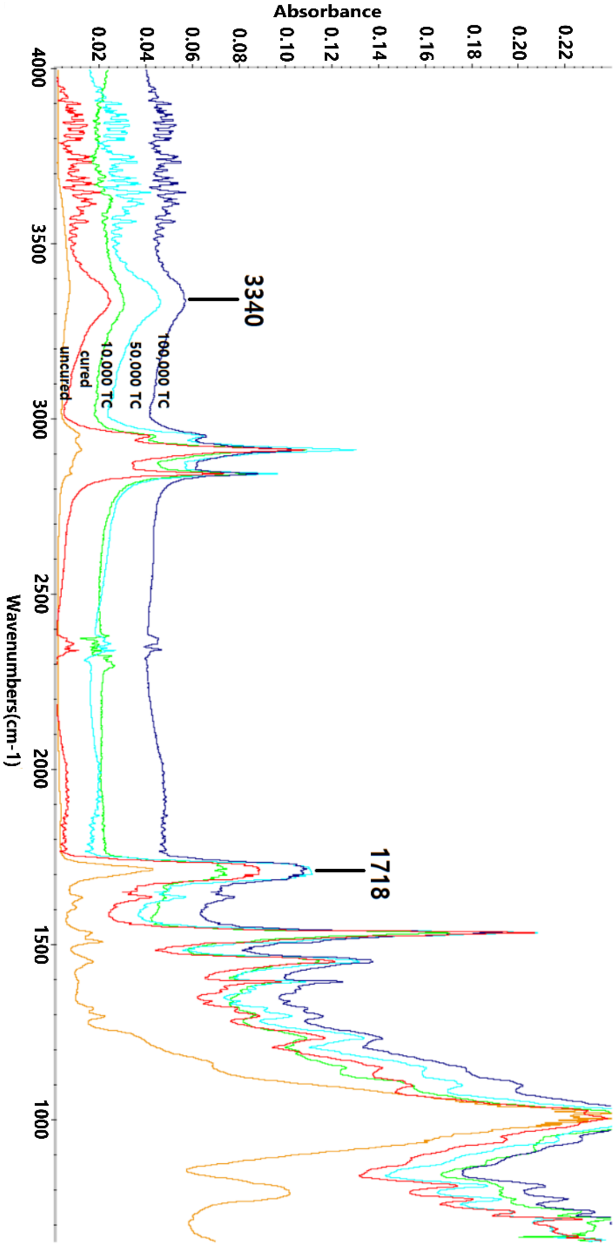

Figure 5. FTIR-ATR peaks of Z250 samples in DW. The ester peak in Bis-GMA also has a carboxylic peak in addition to the ester peak; as a result, the peak (1718 cm^{-1}) appears broad from 1730 cm^{-1} and 1700 cm^{-1}. The OH peak in Bis-GMA can be observed around 3340 cm^{-1}.

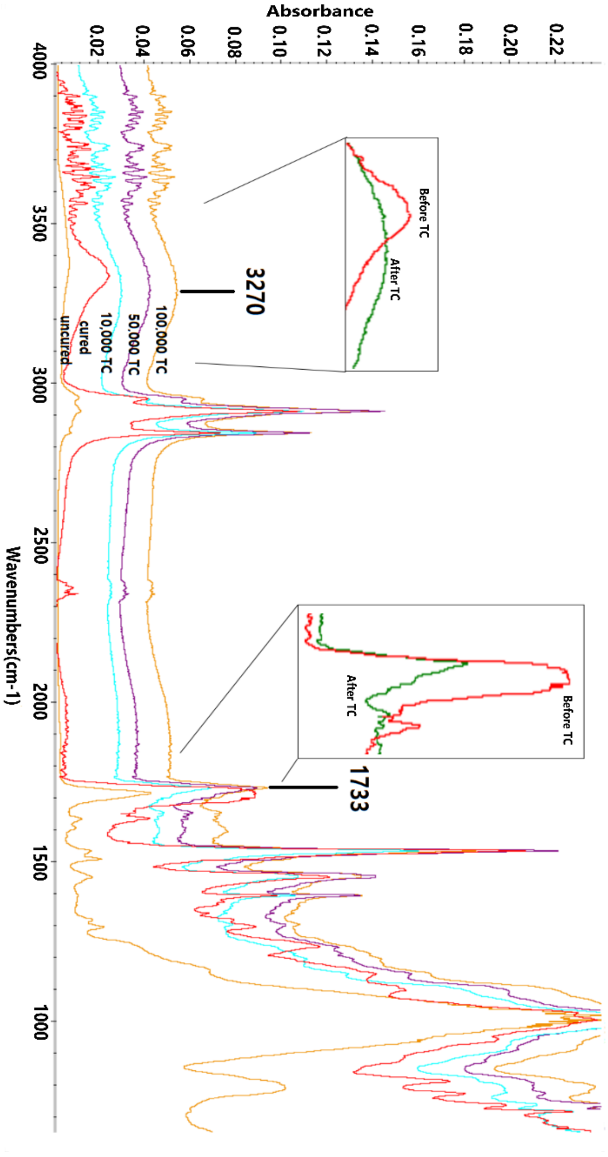

Figure 6. FTIR−ATR peaks of Z250 samples in Coca−Cola. The −OH peak observed at 3340 cm^{-1} in DW (red in the left box) was lowered and shifted to 3270 cm^{-1} (green). The 1718 cm^{-1} peak, which appeared relatively wide in DW (red in the right box), was shifted to 1733 cm^{-1} and became sharper (green).

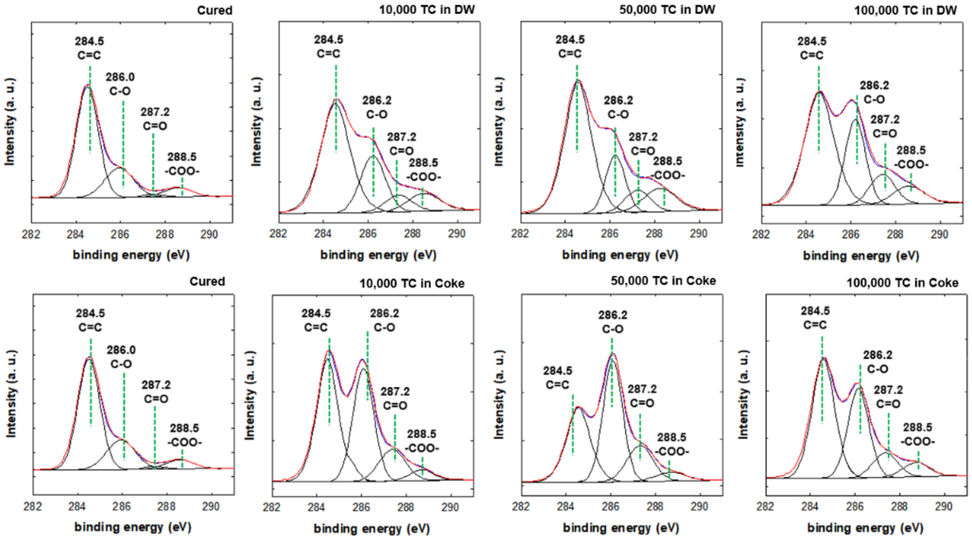

Figure 7. Deconvoluted C1s peaks showing their component peaks in Z250 resin–based composite. When the number of cycles increased, the intensity of the C1s (C=C) peak decreased relatively compared to that of the C1s (C–O) peak in both conditions. In the DW conditions, the intensity of the C–O peak relative to that of C=C peak gradually increased with the number of cycles; however, in Coca–Cola conditions, that of the C–O bond relative to that of C=C peak increased rapidly.

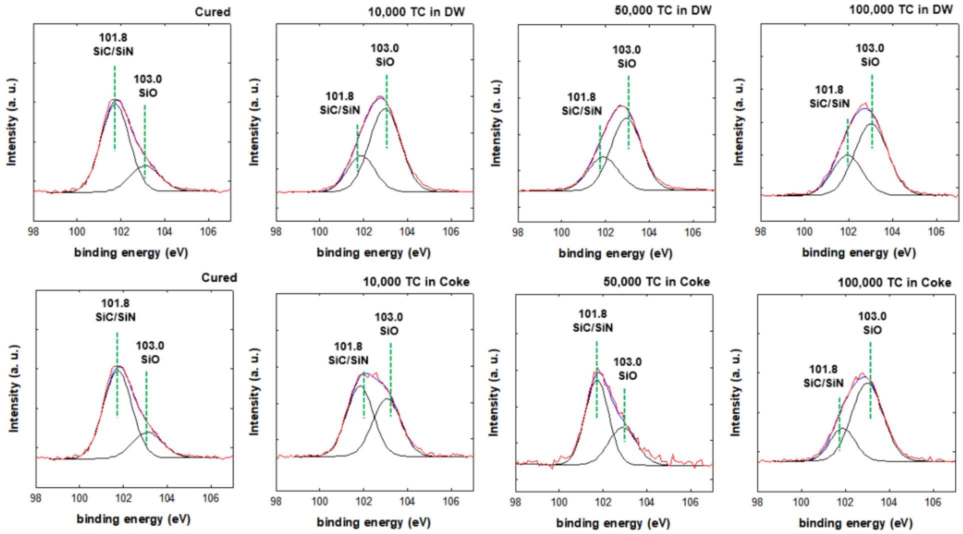

Figure 8. Deconvoluted Si2p peaks showing their component peaks in Z250 resin−based composite.

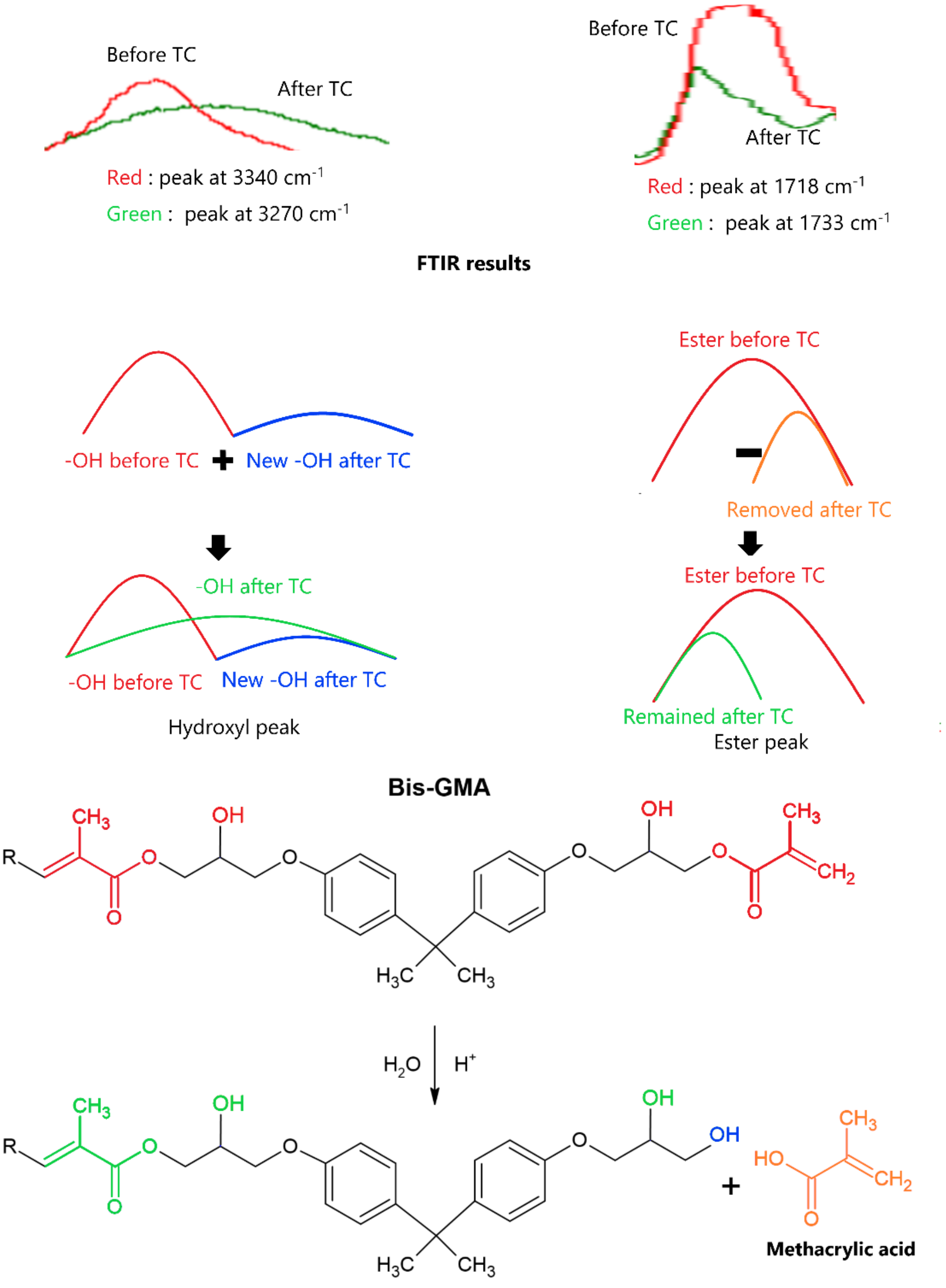

Figure 9. Schematic illustration of the shape and shift of the hydroxyl and ester peaks, wherein multiple bonding energies may be merged to form a peak (Upper illustration).

Middle illustration: Methacrylic acid (MA, orange) is washed out and removed from the surface, which narrows and shifts the ester peak (from red to green in the upper-right illustration). In contrast, the other end of the hydrolyzed Bis-GMA (Bis-HPPP) changes to an -OH group (blue) and adds another -OH peak to the spectrum, making the peak shift and broaden (from red to green in upper-left illustration). Lower illustration: Mechanism of hydrolysis of Bis-GMA. During thermocycling at 55° C, the large amount of H+ contained in the Coca-Cola can hydrolyze Bis-GMA into bishydroxy-propoxy-phenyl-propane (Bis-HPPP) and MA.

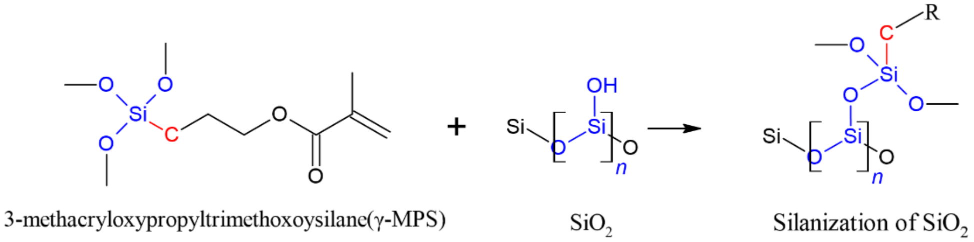

Figure 10. Silanization process of SiO_2 with γ−MPS. In XPS, the bonds shown in red are observed as Si−C peaks and those shown in blue are observed as Si−O peaks.

국문 초록

열순환 처리가 산성환경에서 복합레진의 기계적, 화학적 변화에 미치는 영향

강승호

서울대학교 대학원

치의과학과 치과보존학 전공

(지도교수 조 병 훈)

1. 목적

본 연구의 목적은 복합레진과 지오머가 산성환경에 장기간 노출되었을 때, 굽힘강도의 변화를 관찰하고, 화학적 분석을 통해 그

변화의 원인을 규명하고자 하였다.

2. 재료 및 방법

제작한 시편들(2 mm × 2 mm × 25 mm)을 두가지 환경(증류수[DW], pH 7.0; 코카콜라, pH 2.4-2.8) 에서 다양한 횟수로 열순환을 가하여 노화시켰다. 열순환 처리된 시편들에 대해 만능시험기(LF Plus, Lloyd Instruments, Fareham, UK)에서 4점 굴곡시험을 시행하였다. 압력을 받아 파절된 부위와 그 아래쪽부분을 주사전자현미경(SEM, Apreo S, Thermo Fisher Scientific, Waltham, MA, USA)으로 촬영하여 표면을 관찰하였다. 열순환 횟수(0회, 1만회, 5만회, 10만회)에 따라 총 네 번의 Fourier transform infrared spectroscopy(FTIR) 스펙트럼을 attenuated total reflectance(ATR) mode로 측정(FTIR-ATR, Spectrum 100, PerkinElmer, Waltham, MA, USA)하여 Z250의 흡수 스펙트럼의 변화를 관찰하였다. XPS(K-Alpha+, ThermoFisher Scientific, Waltham, MA, USA) 분석은 화학적 변화를 비교하기 위해 파절이 일어나는 인장응력이 작용한 Z250의 바닥면에서 측정하였다. 굴곡강도 데이터는 3원 분산분석으로 통계적 분석 후 Tukey 사후검정을 시행하였다. 유의 수준은 5%로 설정하였다.

3. 결과

증류수 환경에서 Tetric N-Ceram과 지오머인 Beautifil II는 1만회

열순환 이후 굴곡강도의 변화는 없었으나, 이후 10만회까지 지속적으로 감소하였다($p<0.05$). Z250의 초기 굴곡강도는 Tetric-N-Ceram과 Beautifil II의 굴곡강도에 비해 높지만, 5만회의 열순환까지 지속적으로 감소하지만($p<0.05$), 이후 10만회까지 추가적 감소는 없었다. 콜라에서는 증류수에서와는 다르게 Tetric N-Cream과 Beautifil II는 1만회 열순환 이후 급격하게 굴곡강도가 감소하였다($p<0.05$). 1만회까지 감소한 이후 10만회까지는 통계적 차이가 나는 변화는 없었다. 그러나 Z250은 10만회 열순환 이후 두 조건 모두에서 약간의 상승이 나타났다($p<0.05$). SEM 촬영 결과, 열순환 횟수가 증가할수록 다공성이 증가하고 불규칙한 모양의 필러들이 더 많이 관찰되었다. 같은 횟수의 열순환을 했을 때, 증류수보다 콜라에서 더 많은 다공성이 관찰되었다. FTIR-ATR을 사용하여 3340 cm^{-1}에서 관찰되는 하이드록실기와 1730-1700 cm^{-1} 에서 관찰되는 에스터기의 변화를 관찰하였다. 증류수에서는 열순환 이후에도 별다른 변화가 관찰되지 않았다. 코카콜라에서는 열순환 이후 3340 cm^{-1} 의 하이드록실기 피크가 3270 cm^{-1}으로 이동하였고, 기존 피크보다 좀더 넓고 완만한 경사를 보였다. 1730-1700 cm^{-1}에서 관찰되는 에스터기는 피크가 1733 cm^{-1}로 이동하였고, 기존보다 좁고 날카로운 모양의 피크로 변화하였다. XPS에서는 열순환 이후 C=C 피크의 감소와 C-O 피크의 증가가 공통적으로 관찰되었다. 증류수에서 Si-O 피크는 Si-C 피크에 비해 점진적으로 증가하였으며 콜라에서는 Si-O 피크가 증가하지만, 점진적이지 않았고 10만회 이후에는 증류수와 비슷해졌다.

4. 결론

증류수에서 열순환을 시행하면, 미반응 단량체와 계면결착제가 씻겨나가고 다공성과 굴곡감도의 감소가 나타난다. 코카콜라에서는 산성환경이 레진기질의 에스터기에 가수분해를 촉진시켜 더 많은 다공성을 나타내고 더 빠른 굴곡강도의 감소가 나타난다.

주요어 : 열순환; 화학적 변화; 굴곡강도; 복합레진; 표면조도

학번 : 2019-30042